Journal of Neurochemistry

JNC

JOURNAL OF NEUROCHEMISTRY | 2013

doi: 10.1111/jnc.12395

ORIGINAL ARTICLE

Urban air pollutants reduce synaptic function of CA1 neurons via an NMDA/NO· pathway *in vitro*

David A. Davis,* Garnik Akopian,* John P. Walsh,* Constantinos Sioutas,† Todd E. Morgan* and Caleb E. Finch*,‡

*Davis School of Gerontology, University of Southern California, Los Angeles, California, USA

†Viterbi School of Engineering, Dornsife College, University of Southern California, Los Angeles, California, USA

‡Department of Neurobiology, Dornsife College, University of Southern California, Los Angeles, California, USA

Abstract

Airborne particulate matter (PM) from urban vehicular aerosols altered glutamate receptor functions and induced glial inflammatory responses in rodent models after chronic exposure. Potential neurotoxic mechanisms were analyzed *in vitro*. In hippocampal slices, 2 h exposure to aqueous nanosized PM (nPM) selectively altered post-synaptic proteins in cornu ammonis area 1 (CA1) neurons: increased GluA1, GluN2A, and GluN2B, but not GluA2, GluN1, or mGlur5; increased post synaptic density 95 and spinophilin, but not synaptophysin, while dentate gyrus (DG) neurons were unresponsive. In hippocampal slices and neurons, MitoSOX red fluorescence was increased by nPM, implying free radical production. Specifically, NO· production by slices was increased within 15 min of exposure to nPM with dose dependence, 1–10 μg/mL. Correspondingly, CA1 neurons exhibited increased nitrosylation of the GluN2A receptor and dephosphorylation of GluN2B (S1303) and of GluA1 (S831 & S845). Again, DG neurons were unresponsive to nPM. The induction of NO· and nitrosylation were inhibited by AP5, an NMDA receptor antagonist, which also protects neurite outgrowth *in vitro* from inhibition by nPM. Membrane injury (EthidiumD-1 uptake) showed parallel specificity. Finally, nPM decreased evoked excitatory post-synaptic currents of CA1 neurons. These findings further document the selective impact of nPM on glutamatergic functions and identify novel responses of NMDA receptor-stimulated NO· production and nitrosylation reactions during nPM-mediated neurotoxicity.

Keywords: air pollution, CA1 neurons, glutamate, nitric oxide, nitrosylation, NMDA.

J. Neurochem. (2013) 10.1111/jnc.12395

Urban air pollution adversely impacts brain functions in human populations and animal models. Emerging findings show associations of airborne pollutant levels with mild cognitive impairments (Calderon-Garciduenas *et al.* 2008; Chen and Schwartz 2009; Power *et al.* 2011, 2013; Weuve *et al.* 2012). Brains from a highly polluted city had premature inflammation and neurodegeneration (Block and Calderon-Garciduenas 2009). Rodents chronically exposed to particulate matter (PM) from diesel engines or urban traffic emissions also developed glial inflammatory responses (Kleinman *et al.* 2008; Levesque *et al.* 2011a,b, 2013; Morgan *et al.* 2011; Win-Shwe and Fujimaki 2011) and oxidative stress with protein nitrosylation (Levesque *et al.* 2011b) and lipid peroxidation (Zanchi *et al.* 2010). Exposure of rats to diesel exhaust also impaired memory functions associated with the hippocampus (Fonken *et al.* 2011; Win-Shwe *et al.* 2012).

The basis for hippocampal memory impairments from inhalation of urban air pollutants could include glutamate receptors, which are altered in rodent models by exposure to nPM from diesel exhaust (Win-Shwe *et al.* 2009) or by nPM

Received April 2, 2013; revised manuscript received June 27, 2013; accepted July 29, 2013.

Address correspondence and reprint requests to Caleb E. Finch, 3715 McClintock Avenue, University of Southern California, Los Angeles, CA 90089, USA. E-mail: cefinch@usc.edu

Abbreviations used: AMPA, α-amino-3-hydroxy-5-methyl-4-isoxazolepropionic acid; AP5, D,L-2-amino-5-phosphonopentanoic acid; CA1, cornu ammonis area 1; DG, dentate gyrus; EPSC, excitatory postsynaptic current; EthD-1, ethidium homodimer-1; GluA1, glutamate receptor AMPA subunit 1; GluN2A/B, glutamate receptor NMDA subunit; mGluR, metabotropic glutamate receptor; NMDA, *N*-methyl-D-aspartic acid; NO·, nitric oxide; nPM, nanoscale particulate matter; PSD95, Post Synaptic Density 95.

of < 0.2 μm fractioned from Los Angeles urban freeway air in our prior study (Morgan *et al.* 2011). The nano-sized PM (ultrafine PM) from combustion engines has consistently shown higher toxicity than larger PM *in vivo*, e.g. (Li *et al.* 2013) and *in vitro* (Li *et al.* 2003; Gillespie *et al.* 2013). Inhalation of nPM for 150 h during 10 weeks decreased hippocampal levels of the GluA1 subunit of AMPA receptors (Morgan *et al.* 2011). The selectivity of responses to nPM is indicated by the absence of changes in GluA2 levels or in the associated synaptic proteins post synaptic density 95 (PSD95) or synaptophysin.

In vitro primary hippocampal neuronal cultures also showed inhibition of neurite outgrowth during exposure to nPM at 2 μg/mL for 48 h, an effect rescued by the NMDA receptor antagonist AP5 (Morgan *et al.* 2011). nPM induced lactate dehydrogenase release by hippocampal slice cultures, a measure of cell damage, which was also rescued by AP5. Inhibitory effects of nPM on neurite outgrowth may share mechanisms with the regression of hippocampal cornu ammonis area 1 (CA1) and CA3 dendrites after *in vivo* exposure to vehicular-derived PM of 2.5 μm size (Fonken *et al.* 2011).

To further analyze the mechanisms of nPM on glutamatergic functions, we examined the effects of acute nPM on synaptic proteins in hippocampal slices and dissociated neurons. nPM cross cell membranes by non-phagocytic mechanisms (Geiser *et al.* 2005) consistent with their relatively high hydrophobicity (Xia *et al.* 2006). Because nPM rapidly induced free radicals in macrophages (Li *et al.* 2003; Xia *et al.* 2006), we investigated free radical production in slices and neuronal cultures, with emphasis on nitric oxide ($NO^{\cdot}$). Glutamatergic subunit nitrosylation was examined because NMDA receptors are vulnerable to oxidative damage (Aizenman *et al.* 1989, 1990; Manzoni *et al.* 1992; Shi *et al.* 2013). Neuronal selectivity was assessed by comparing effects of nPM on CA1 pyramidal neurons, which are more vulnerable than DG neurons to nPM toxicity (Fonken *et al.* 2011), ischemia (Kawasaki *et al.* 1990), and Alzheimer disease (Morrison and Hof 1997). To evaluate functional outcomes of nPM, synaptic transmission was examined by patch clamp recording.

Material and methods

Animals

Male C57BL/6J mice (1 month) were purchased from Jackson Laboratories (Sacramento, CA, USA) and pregnant Sprague–Dawley rats from Harlan Labs (Livermore, CA, USA). Animals were maintained and treated using animal procedures conforming to NIH guidelines as approved by the USC Institutional Animal Care & Use Committee (IACUC). Animals were killed after isoflurane anesthesia.

nPM collection

Nanoscale particulate matter (nPM < 200 nm) was collected continuously for 30 days in a well-studied site in downtown Los Angeles next to the CA-I110 Freeway (Sardar *et al.* 2005), which has a yearly average of 10.5 ± 2.9 ug/m^3, ranging 6.1 to 15.6 ug/m^3 across months (Daher *et al.* 2013). Using a High-Volume Ultrafine Particle (HVUP) Sampler at 400 L/min (Misra *et al.* 2002; Ning *et al.* 2007), nPM was trapped on Teflon filters (20 × 25.4 cm, PTFE, 2 μm pore; Pall Life Sciences, Port Washington, NY, USA). nPM was then transferred to sterile aqueous suspension by vortexing and sonication, with differential elution of components (Morgan *et al.* 2011) (see Discussion below). Aqueous suspensions of nPM pooled from 30 days of collection as stocks of ca. 200 μg/mL, which were aliquoted and stored at −20°C. The frozen stocks retain markers of chemical stability for > 3 months (Li *et al.* 2003; Morgan *et al.* 2011). Endotoxin was not detected in nPM stocks (Limulus amoebocyte assay) (Lonzo Biologics, Hopkinton, MA, USA).

Acute hippocampal slices

Slices were prepared from 1-month-old male mice in ice-cold modified artificial cerebrospinal fluid (aCSF) containing 124 mM sucrose, 62 mM NaCl, 3 mM KCl, 3 mM $MgCl_2$, 1.25 mM $CaCl_2$, 26 mM $NaHCO_3$, 1.25 mM NaH_2PO_4, 10 mM glucose. Transverse hippocampal slices (400 μm) were cut by a Vibratome-1000 (Vibratome Co., St Louis, MO, USA) or a McIlwain tissue chopper (Brinkmann Instruments Inc., Westbury, NY, USA). Slices were transferred to aCSF (124 mM NaCl, 3 mM KCl, 1.5 mM $MgCl_2$, 2.5 mM CaCl2, 26 mM $NaHCO_3$, 1.25 mM NaH_2PO_4, 10 mM glucose), with pre-incubation for 30 min at 30°C. The aCSF was continuously bubbled with 95% O_2/5% CO_2 in the standard electrophysiological paradigm (see below). Following pre-incubation, slices from three to four brains were transferred to fresh aCSF (10 slices per 20 mL) at 22°C, to which nPM suspensions were added. Some experiments included the NMDA antagonist AP5 (D, L-2-amino-5-phosphonopentanoic acid; Sigma Chemical Corp., St. Louis, MO, USA). After 2-h incubation, slices were prepared for patch clamp electrophysiology recordings or western blot (see below).

Dissociated hippocampal neuronal cultures

Primary hippocampal neuronal cultures were derived from embryonic day 18 (E18) rats. Briefly, hippocampi were dissociated in Hank's balanced salt medium containing trypsin and DNase at 37°C (Banker and Cowan 1977). Dissociated cells were plated on poly-D-lysine and laminin coated glass coverslips (20 000 cell/cm^2), or on 96-well plates (70 000 cell/cm^2); media were Dulbecco's modified Eagle's medium (DMEM), supplemented with B27 (Invitrogen, Grand Island, NY, USA). Neurons were cultured for 7 or 14 days at 37°C with 5% CO_2 and exposed to nPM and AP5 (50 μM) for 2 h.

Electrophysiology

After exposure to the nPM suspension or control aCSF (2 h/22°C), individual hippocampal slices were transferred to a recording chamber at 35°C (Akopian *et al.* 2008) and superfused with aCSF at 2 mL/min. Individual CA1 pyramidal neurons were recorded by standard whole-cell voltage clamp methods (Akopian and Walsh 2002) (See Fig. 5a). Evoked synaptic currents were recorded using a Multiclamp 700B amplifier and Digidata 1440A (Molecular Devices, Sunnyvale, CA, USA). Patch pipettes were filled with 120 nM $CsMeSO_4$, 10 mM CsCl, 5 mM EGTA, 2 mM $MgCl_2$ 10 mM HEPES, 5 mM QX-314 (Sodium channel inhibitor), 2 mM

ATP-Mg, 0.25 mM GTP-Na, pH 7.25, 285 mOsm, and spermine (0.1 mM). Resistance ranged from 2 to 4 MΩ.

CA1 pyramidal cells were identified under IR illumination. Passive membrane properties were determined in voltage clamp mode with the 'Membrane Test' option of the Clampex 10 software (Molecular Devices) by 10 mV depolarizing voltage steps. Series resistance (Rs) was compensated up to 80%. Schaffer collaterals were stimulated by a glass pipette (1 mM NaCl) 100–150 μm from the recorded CA1 neurons. Extracellular stimulation was generated with Master 8 pulse generator, delivered by Iso-Flex stimulus isolation unit (AMPI, Jerusalem, Israel).

Synaptic input-output (I/O) curves of synaptic currents were obtained by stimulating stratum radiatum of each slice with ascending stimulus intensities (5–25 μA). I/O curves were plotted as amplitudes of evoked excitatory post-synaptic currents (EPSCs) versus stimulus intensities of evoked EPSCs. The paired-pulse ratio (PPR) was estimated from the average of five paired-pulse synaptic stimulations with interstimulus intervals of 50 ms every 20 s. Cells were voltage-clamped at a membrane potential of −60 mV. The PPR (% of the ratio of the second pulse to the first) estimated changes in pre-synaptic release. The I/O and PPR of CA1 neurons were based on six to seven neurons measured per condition.

Free radicals

Free radical production was estimated in slices or neurons after 2 h of nPM (10 μg/mL) by MitoSox™ Red (Molecular Probes, Grand Island, NY, USA); MitoSox (2.5 μm) was added to aCSF (slices) or DMEM (neurons) for 15 min (Ma *et al.* 2011). Fluorescent intensity was quantified in neuronal perikarya by ImageJ software (National Institute of Health, Bethesda, MD, USA) (Fig. 3a and Figure S4) and expressed as the mean fluorescent intensity per neuron (N = 3–4 cultures per condition) or per hippocampal region (N = 7 slices per condition).

For nitric oxide ($NO^{\cdot}$), acute slices were incubated in aCSF (see above) with nPM for 15–60 min. Media were analyzed spectrophotometrically for $NO^{\cdot}$ as nitrite by the Griess reagent [0.1% v/v *N*-(1-naphthyl) ethylenediamine dihydrochloride, 1% v/v sufanilamide, and 2.5% v/v phosphoric acid; (Sigma)](Ignarro *et al.* 1993; Xie *et al.* 2002) using $NaNO_2$ as a standard and normalized to background [nitrite] in aCSF; four to six experiments per condition (N = 10 slices per experiment).

Cell viability

Cell viability was assessed in hippocampal slices (N = 8–12 per condition) by the LIVE/DEAD® assay (Molecular Probes) (Stein *et al.* 2004). After incubation with nPM, 2 μM Calcein AM and 4 μM EthD-1 were added for 15 min. Wet mounts of slices were directly imaged. EthD-1 positive cells were enumerated in hippocampal regions using Image J software. For primary cultures (N = 21–38 per experiment), neurons were co-stained with Calcein AM (Molecular Probes, viable cells) and EthD-1 (injured cells). Viability was expressed as the ratio of injured cells to viable cells.

Immunochemistry

Following nPM treatment, acute hippocampal slices, and neuronal cultures were fixed with 4% v/v paraformaldehyde in phosphate buffered saline pH 7.4 (PBS). Subsequently, slices were submerged in 30% sucrose/PBS pH 7.4, then embedded in OTC before sectioning on a cryostat. Tissue sections (30 μm) were permeablized with 1% NP-40/PBS and immunoprobed for 2 h at 22°C for markers of neurons (NeuN), astrocytes (GFAP), and microglia (Iba1) (Table S1). Immunofluorescence was visualized using Alexa Fluor® antibodies (Molecular Probes). For primary cultures, coverslips were washed and permeablized with 0.2% triton x-100 then immunoprobed with antibodies against glutamate receptors (GluA1, GluN2b) and synaptic proteins (PSD95, spinophillin, synaptophysin) overnight at 4°C (Table S1).

Receptor proteins

After incubation (see above), hippocampal slices were microdissected on a chilled platform into two portions containing the CA1 and DG neuronal regions, with excision of the CA2/3 pyramidal neuron layer and the subiculum. Three microdissected slices per condition were pooled and homogenized in Radioimmunoprecipitation assay buffer (EMD Millipore, Billerica, MA, USA) by a teflon pestle, followed by centrifugation 10 000 *g*/10 min at 4°C. Total supernatant protein concentration was assayed by BCA (Thermo Scientific, Rockford, IL, USA) with bovine serum albumin (BSA) as a standard. For western blots, 15–20 μg of protein in Laemmli loading buffer (Boston BioProducts, Ashland, MA, USA) was electrophoresed on 8% sodium dodecyl sulfate-polyacrylamide gels, and then by transferred to polyvinylidene fluoride membranes (EMD Millipore). Membranes were blocked in 5% BSA for 1 h, and then probed with primary antibodies against AMPA receptor subunits (GluA1, GluA2), metabotropic receptor (mGluR5), NMDA receptor subunits (GluN1, GluN2A, GluN2B), and synaptic proteins (PSD95, spinophillin, synaptophysin) overnight at 4°C, then incubated with secondary antibodies conjugated with an infrared dye (LI-COR Biosciences, Lincoln, NE, USA) (Table S1). Protein levels were analyzed by densitometry using synaptophysin or actin as a loading control as the average of three to four experiments, with three to four wells per condition (CTL, nPM).

To measure post-translational modifications on CA1 proteins, membranes were first probed with antibodies to detect S-nitrosylation (SNO-cysteine) or phosphorylation (GluA1, S831 & S845; GluN2B, S1303). After detection, membranes were stripped and reprobed with antibodies for total proteins. Nitrosylation and phosphorylation were expressed as the ratio of modified to total levels. The specificity of nitrosylation was confirmed by immunoprecipitation of the protein extract (0.1 mL, 1 mg/mL) with 10 μg of antibodies to GluN2A or GluA1, using protein g-Sepharose beads (Pierce, Thermal Scientific, Rockford, IL, USA) (Ryan *et al.* 2013); after incubation for 2 h/4°C, the bead-bound proteins were collected by centrifugation (800 g × 10 min), washed in Radioimmunoprecipitation assay buffer, and eluted at 99°C/5 min in Laemmli loading buffer, followed by electrophoresis and western blotting.

Statistics

Statistical analysis used Prism Version 5 (Graph Pad, La Jolla, CA, USA) and Clampfit 10 software (Molecular Devices). Multiple comparisons used ANOVA with Tukey post-test. Single comparison used Student's t-test. Data are expressed as mean ± SEM; significance level of alpha = 0.05.

Results

Glutamate receptor subunit modification

Following 2-h incubation of mouse hippocampal slices in 10 μg/mL nPM, the CA1 and DG neuronal regions were analyzed for glutamate receptor subunits and synaptic proteins (Figs 1 and 2, Table S2). The western blot bands corresponded to expected sizes (Figure S1). In the CA1 region, levels of NMDA receptor subunits were increased selectively: GluN2A (+60%) and GluN2B (+80%) (Fig. 1a and b), whereas GluN1 levels did not change (Fig. 1c). AMPA receptor subunits also responded selectively with increased GluA1 (+70%) (Fig. 1d), but no change in GluA2 (Fig. 1e) or in the metabotropic receptor GluR5 (Fig. 1f). DG neurons did not show these receptor protein responses (Figure S1; Table S2).

Receptor phosphorylation per subunit was decreased by nPM exposure: GluN2B (NMDA subunit) at S1303 (-30%) (Fig. 1g) and GluA1 at S831 and S845 (−40%) (Fig. 1h and i). Post-synaptic proteins associated with NMDA receptors were increased: PSD95 (+100%) (Fig. 2a), spinophilin (+50%) (Fig. 2b); there were no changes in synaptophysin (Fig. 2c) or NeuN (Fig. 2d). Astrocyte GFAP and microglial/macrophage CD11b were also unchanged by 2 h nPM treatment (not shown).

To further document acute nPM selectivity on pyramidal neurons these findings were extended to dissociated rat hippocampal neurons in culture by immunocytochemistry (Figure S3). nPM increased levels of GluN2B (+20%) (Figure S3a) as in slices; however, GluA1 decreased (−20%) (Figure S3b), which is in the opposite direction from the slice response. Other responses of neurons paralleled those of slices: PSD95 (+20%) (Figure S3c) and spinophilin (+30%) (Figure S3d), but not synaptophysin (Figure S3e). The phosphorylation of GluN2B (S1303) and GluA1 (S831 & S845) was also decreased (not shown). These responses were attenuated by AP5 (NMDA receptor antagonist) in cultured neurons, whereas in slices AP5 did not consistently attenuate nPM effects on total receptor subunit levels.

Free radicals and nitrosylation

Because excessive glutamatergic function increases oxidative stress (Reyes *et al.* 2012) and because nPM increased free radical production in monocytic cells (Li *et al.* 2003; Xia *et al.* 2006), we evaluated oxidant levels with MitoSOX™ red, a mitochondrially targeted ethidium dye that was responsive to increased superoxide and other oxidants induced in lung epithelial cells by urban PM (Zhao *et al.* 2009). In both hippocampal slices (Fig. 3) and dissociated primary neurons (Figure S3), nPM induced MitoSox fluorescence by 40–50%. Hippocampal neuronal layers gave stronger signals than adjacent neuropil (Fig. 3). In dissociated neurons, response to nPM was consistently blocked by AP5 (Figure S2), whereas slice responses to nPM + AP5 were inconsistent (not shown).

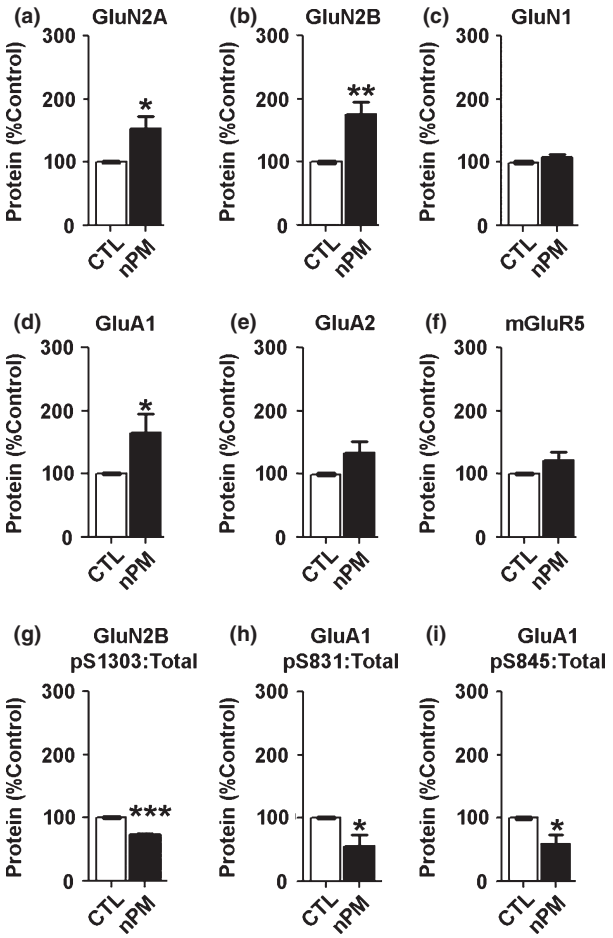

Fig. 1 Glutamate receptor protein responses to acute nanosized particulate matter (nPM). Western blots of lysates from the cornu ammonis area 1 (CA1) region of mouse hippocampal slices, microdissected after incubation with nPM (10 μg/mL, 2 h) (a–c) NMDA subunits: (a) GluN2A (+60%); (b) GluN2B (+70%); (c) GluN1, no change; (d–e) AMPA subunits: (d) GluA1 (+70%), (e) GluA2, no change; (f) mGluR5, no change; (g–i) Receptor phosphorylation: (g) GluN2B, pSer1303 (−30%); (h) GluA1, pS831 (−40%); (i) GluA1 pS845 (−40%). Each panel represents the average of three to four experiments, with three to four wells per condition (CTL, nPM), each containing three slices. Values from blots were normalized for synaptophysin, which is unchanged by nPM (Fig. 2). Data are expressed as % CTL per experiment. *$p < 0.05$; **$p < 0.01$; ***0.0001.

Nitric oxide ($NO^{\cdot}$) was a candidate for free radical responses because inhalation of diesel exhaust particles increased brain protein nitrotyrosine (Levesque *et al.* 2011b). $NO^{\cdot}$ in hippocampal slices exposed to nPM (1, 5, 10 μg/mL) was increased by 20-fold within 15 min (Fig. 4a). Again, the induction was blocked by AP5 (Fig. 4b). Correspondingly, there were 50% increases of S-nitrosylation of cysteine residues on GluN2A and GluA1 (Fig. 4c). The specificity of

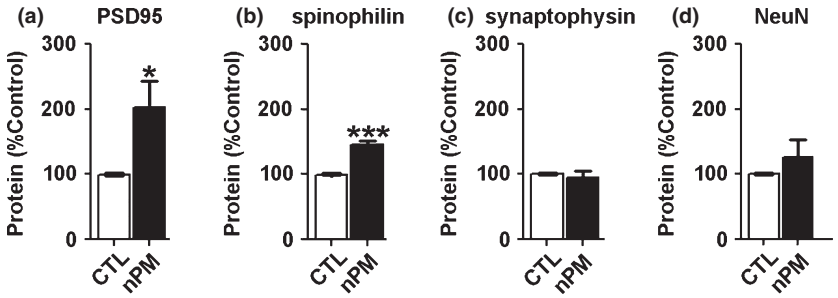

Fig. 2 Cornu ammonis area 1 (CA1) synaptic protein response to acute nanosized particulate matter (nPM). Synaptic and nuclear proteins (western blot) of the microdissected CA1 region of mouse hippocampal slices incubated with nPM (10 μg/mL, 2 h) (a–b) Post-synaptic: (a) Post synaptic density 95 (+100%); (b) spinophilin (120 kDa and 96 kDa, total and cleaved) (+40); (c) Pre-synaptic: synaptophysin (no change); (d) NeuN (neuronal nuclear protein) (no change); Data were obtained and expressed as described in Fig. 1. $^{*}p < 0.05$; $^{***}p < 0.001$.

glutamate receptor nitrosylation was further documented by immunoprecipitation (Figure S3). GAPDH nitrosylation was also increased (+50%) (Fig. 4c). Protein s-nitrosylation was greatest in the CA1 region (Table S2). By ethidium uptake (EthD-1), neuronal membrane damage was greater in CA1 than in DG (Fig. 4d). In cultured neurons, EthD-1 uptake showed dose-dependent increase in response to nPM, again blocked by AP5 (Figure S4).

Effects of nPM on excitatory post-synaptic currents

Functional consequences of these biochemical changes were explored by analyzing EPSCs in hippocampal slices (Fig. 5a). Exposure to nPM (10 μg/mL, 2 h) reduced EPSC amplitudes by about 50% in CA1 neurons across a range of stimulus intensities (Input/Output, Fig. 5b and c). There were no effects of nPM on CA1 neuron membrane resistance or capacitance (not shown). Moreover, the paired-pulse facilitation of CA3 pre-synaptic Schaeffer collateral terminals was not altered by nPM (Fig. 5d), suggesting that nPM did not alter pre-synaptic transmitter release.

Discussion

We report three new findings on rapid neuronal damage by nPM derived from vehicular traffic using *in vitro* models of acute hippocampal slices and dissociated neurons. (i) Hippocampal slices responded rapidly to nPM with dose-dependent increases of nitric oxide ($NO^{\cdot}$) within 15 min. (ii) Nitrosylation of several glutamate receptor subunits was increased by 2 h, while phosphorylation of other sites was decreased. In both slice and neuronal cultures, levels of post-synaptic proteins PSD95 and spinophilin were increased. Several changes induced by nPM were blocked by the NMDA receptor antagonist AP5. (iii) The amplitude of excitatory post-synaptic currents in CA1 neurons was decreased, while paired-pulse facilitation was unchanged. These findings document that acute exposure to nPM can alter properties of glutamate receptors that are critical to neuronal plasticity and memory processes. These findings suggest mechanisms that contribute to cognitive impairments associated with vehicular-derived pollutants and to the vulnerability of CA1 neurons to excitotoxicity in Alzheimer disease and ischemia (see Introduction).

Dose responses to nPM corresponded to prior studies with these locally derived nPM, in the range of 1–10 μg nPM/mL for *in vitro* brain cell models (Morgan *et al.* 2011) and macrophages (Xia *et al.* 2006). Other PM sources collected from diesel exhaust (Levesque *et al.* 2011b) or from urban Baltimore (Zhao *et al.* 2009) were not as active in cytokine induction at levels < 10 μg/mL on macrophages or bronchial epithelial cells, respectively.

The components of nPM that induced $NO^{\cdot}$ and altered glutamate receptors could include redox active metals, water soluble organic carbon (WSOC), and long-lived free radicals that persist for 30 days after initial collection (Morgan *et al.* 2011). Relative to ambient nPM, the present filter-extracted nPM had similar levels of WSOC and redox active metals, but relatively less black carbon, polyaromatic hydrocarbons, steranes, and organic acids because of differential extraction from filters by sonication (Morgan *et al.* 2011 and its Table S2).

$NO^{\cdot}$ production in hippocampal slice cultures was increased within 15 min of exposure to nPM, followed by nitrosylation of proteins at 2 h. The rapid increase of $NO^{\cdot}$ within 15 min may be the most rapid free radical response to combustion engine-derived PM in refereed reports. For comparison of the time course, macrophages (RAW 264.7 murine line) exposed to 10 μg nPM/mL had increased H_2O_2 production at 30 min (Li *et al.* 2002), followed at 60 min by decreased mitochondrial membrane depolarization ($\Delta\Psi m$), and then increased MitoSox fluorescence at 2 h of exposure; mitochondrial swelling arose by 4 h, followed at 16 h by loss of cristae and increased mitochondrial $[Ca^{2+}]$ (Xia *et al.*

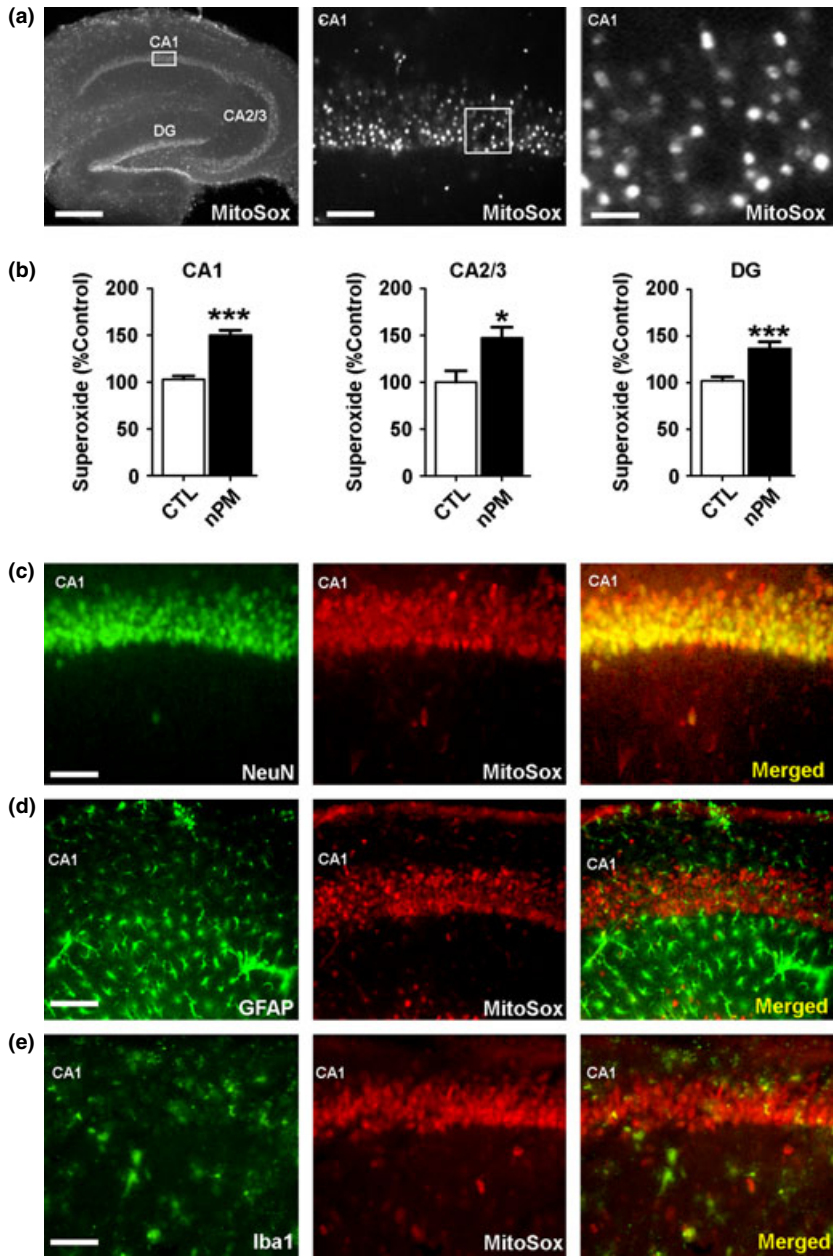

Fig. 3 MitoSox RED oxidant responses to nanosized particulate matter (nPM) in hippocampal slices. Hippocampal slices were incubated with 10 μg/mL nPM for 2 h. (a) Live slice Mitosox™ RED fluorescence; scale bar, 600 μm. Left panel shows intense fluorescence of neuronal layers against weaker signal from the glial rich neuropil. Center and right panels, cornu ammonis area 1 (CA1) neurons at higher magnification; scale bars, 100 and 40 μm. (b) Fluorescence in live slices increased above CTL in all neuronal regions: CA1, +50%, $p < 0.0001$; CA2/3, +45%, $p < 0.01$; DG, +35%, $p < 0.001$. Data are shown as the mean fluorescent intensity by % CTL per hippocampal region ($N = 7$ slices per condition). (c–e) Fixed slices co-stained with Mitosox RED and cell-type markers (green): (c) neurons (NeuN) have much stronger signal than (d) astrocytes (GFAP) and (e) microglia (Iba1); scale bar, 100 μm. *$p < 0.01$; ***$p < 0.001$.

2006). Note that these prior reports used alternate terminology (ultrafine particles, UFP), which were collected at the same site by co-author Sioutas (Morgan *et al.* 2011). Although the size range of UFP was similar to the present nPM, they may have differed in chemical composition because they were not extracted from filters (see above). Since this report was submitted, Gillespie *et al.* (2013) observed increased NO˙ after 24 h incubation of dopaminergic neurons with 8 μg/mL. Responses to nPM may prove to be even faster than 15 min because nPM appear to cross cell membranes directly without endocytosis (Xia *et al.* 2006). Thus, the mitochondrial [Ca^{2+}] influx may begin earlier than the 16-h observation time of Xia *et al.* (2006).

Other reactive oxygen species and oxidants may be induced by nPM besides NO˙. As shown for a different urban PM sample by Zhao *et al.* (2009), we observed that nPM increased the oxidation of mitochondrially targeted hydroethidine (also called MitoSOX™) by about 50%. Although the increased fluorescence of Mito-SOX™ may indicate increased superoxide, it can also be caused by other mitochondrial derived radicals and oxidants (Zielonka and Kalyanaraman 2010). The subsequent induction of the Nrf2-

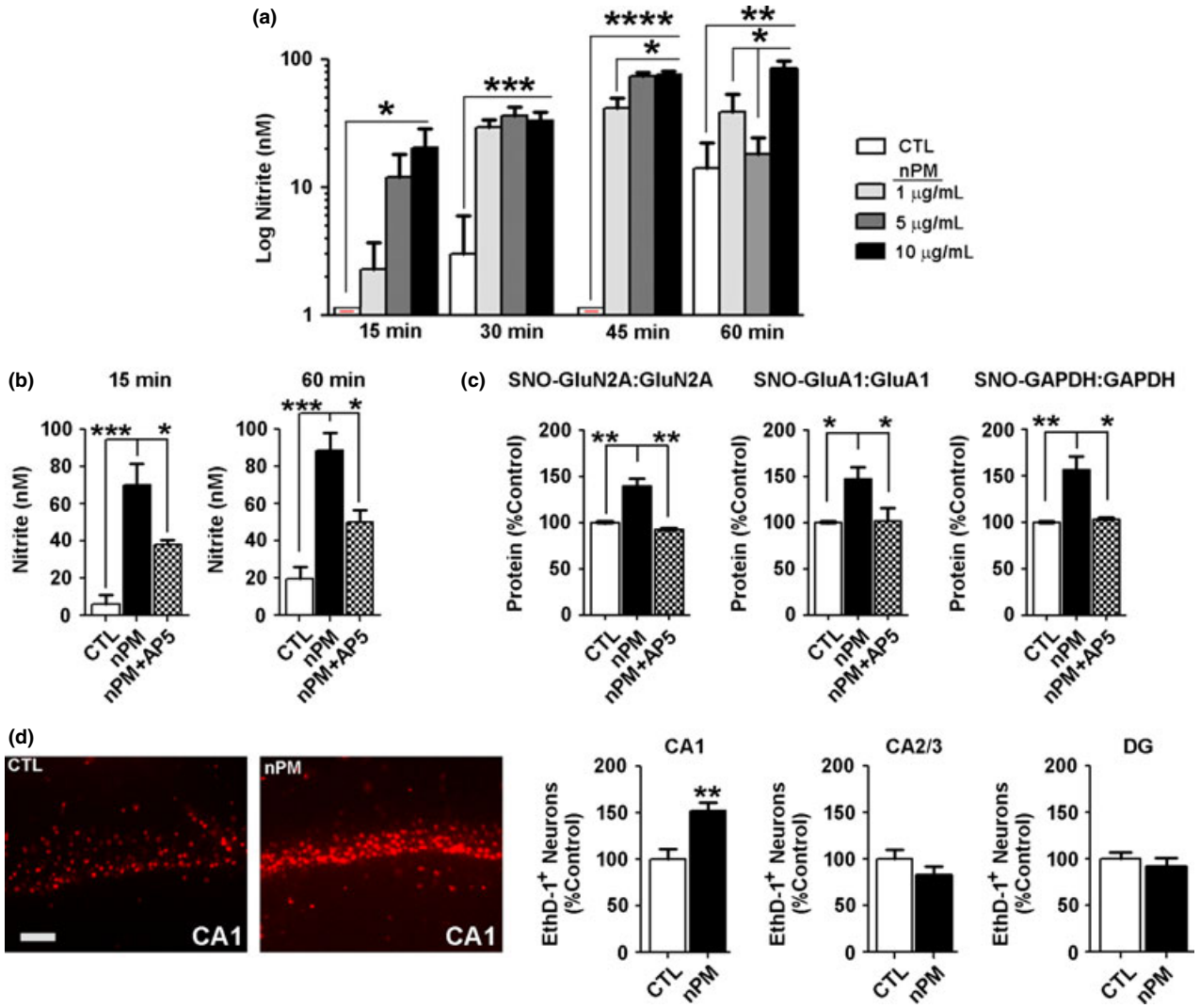

Fig. 4 NO· and protein nitration responses to nanosized particulate matter (nPM). (a) Induction of NO·, assayed as nitrite in the media of mouse hippocampal slices during incubation with nPM at 1, 5, 10 μg/mL, which induced dose-dependent nitrite production at 15–60 min (Griess reaction). (b) AP5 attenuated nitrite increase by 50% after incubation with nPM 10 μg nPM/mL for 15 or 60 min; (c) In whole hippocampal slices, S-nitrosylation of GluN2A, GluA1, and GAPDH (+50%) was increased 40–50% after incubation with 10 μg nPM/mL for 2 h. The increased S-nitrosylation was blocked by AP5. (d) LIVE/DEAD® (EthD-1) uptake as a measure of neuronal injury in hippocampal slices after incubation with 10 μg nPM/mL for 2 h (scale bar, 100 μm): cornu ammonis area 1 (CA1) neurons, +50%; no change in CA2/3 or DG neurons; $*p < 0.05$; $**p < 0.01$; $***p < 0.001$; $****p < 0.0001$.

dependent detoxifying enzymes observed after 10 weeks of *in vivo* exposure (Zhang *et al.* 2012) may thus involve multiple oxidants and free radicals.

In the present acute responses, the blockade of NO· production by the NMDA receptor antagonist AP5 has implications for the mechanisms underlying toxic effects of nPM. Activation of either AMPA or NMDA receptors in hippocampal slices rapidly increased NO· production in CA1 neurons within 5 min (Frade *et al.* 2009). Moreover, NO· production in neurons depended on extra-cellular Ca^{2+} and recruitment of the PSD95/NOS complex to post-synaptic NMDA receptors (Sattler *et al.* 1999). *In vivo*, glutamate and NMDA infusion also rapidly increased NO· levels more in CA1 neurons than DG neurons (Lourenço *et al.* 2011). Further studies are needed to resolve the role of Ca^{2+}, glutamate, and nNOS in the rapid induction of NO· in relation to possible neuronal depolarization by nPM.

Biochemical modifications of glutamate receptor subunits were also observed. The S-nitrosylation of cysteine residues in GluA1 and GluN2A was increased by 50% after 2-h exposure to nPM in CA1; again, DG neurons were unresponsive. The blockade of S-nitrosylation by AP5 is

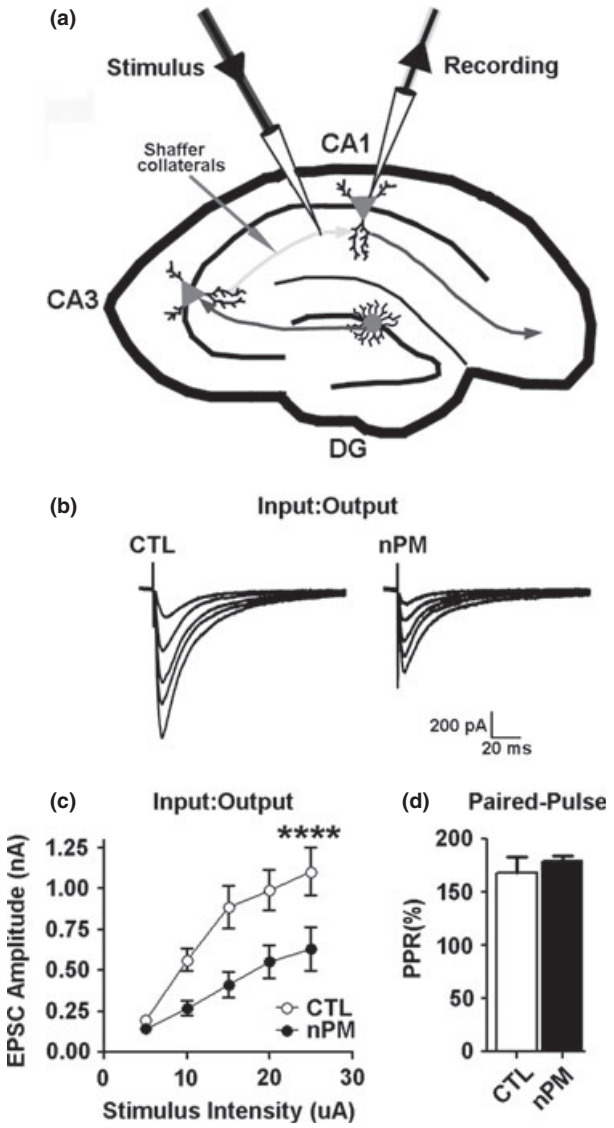

Fig. 5 Nanosized particulate matter (nPM) reduces excitatory synaptic function in cornu ammonis area 1 (CA1) neurons. (a) Schematic of whole cell path clamp recording of CA1 neurons. (b–c) Input/output (I/O) responses of evoked excitatory post-synaptic currents (EPSCs) in CA1 perikarya. (b) EPSC traces from CTL and nPM treated CA1 neurons. (c) An ascending sequence of extracellular stimuli at 20 s intervals was delivered through stimulation of Schaffer collaterals; slices were pre-incubated with 10 μg/mL nPM for 2 h (c) nPM consistently lowered EPSC amplitude (nPM effect, **** $p < 0.0001$). (d) The paired-pulse response (PPR) ratio of pre-postsynaptic terminals in the same slices (50 ms intervals at 15 uA); PPR was not altered by nPM.

consistent with its inhibition of NO˙ induction. Concurrently, nPM decreased phosphorylation of GluA1 (pS831 and pS845) and of GluN2B (pS1303) in slices and neuronal cultures. Because phosphorylation regulates glutamate receptor trafficking to synapses (Santos *et al.* 2009), the decreased phosphorylation in response to nPM could be a factor in the increased levels of GluA1 and GluN2B. However, the opposite directions of nitrosylation and phosphorylation responses to nPM were not predicted by the induction of both nitrosylation and phosphorylation in GluA1 by glutamate agonists, in which phosphorylation of S831-GluA1 required C875 nitrosylation (Selvakumar *et al.* 2013). Further studies may address possible oxidative damage by nPM to cysteines or other residues, which may directly modulate phosphorylation; alternatively, indirect actions through phosphatases or kinases may occur.

By western blots of hippocampal slices, post-synaptic proteins were selectively altered by acute nPM, with increased GluA1 (but not GluA2 or mGluR5), and of GluN2A and GluN2B (but not of GluN1). PSD95 and spinophilin (but not synaptophysin) were also increased. The direction of these changes is consistent with rapid increases of GluN2A and of spine puncta in cultured hippocampal neurons at 70 min after depolarizing pulses of KCl (Baez *et al.* 2013). Notably, these KCl induced increases of GluN2A were blocked by inhibitors of RNA and protein synthesis. Thus, early responses of synaptic protein levels to nPM may be mediated by gene expression as well as by post-translational mechanisms of nitrosylation and phosphorylation.

Cytotoxicity from nPM is also indicated by the nitrosylation of GAPDH measured in whole slice proteins. Excitotoxic glutamate levels also increased GAPDH nitrosylation (Hara *et al.* 2005). By EthD-1 uptake, CA1 neurons showed the greatest membrane damage, which may contribute to their decreased EPSC. This ranking follows the *in vivo* induction of NO˙ by depolarizing KCl to a greater extent in CA1 than DG neurons (Baez *et al.* 2013) and the well-known relative vulnerability of CA1 neurons to ischemia and Alzheimer disease.

Hippocampal neuron cultures responded to nPM in parallel with the hippocampal slices for decreased phosphorylation of GluA1 at S831 and S845. In both slice and neuron cultures, nPM increased PSD95 and spinophilin. In neuron cultures, these responses to nPM were blocked by AP5; because the E18 neurons had limited synapse formation after 7 days of culture, we suggest that AP5 was acting on extrasynaptic NMDA receptors. However, levels of GluA1 protein decreased in cultured neurons, but increased in slices. This divergence may be attributed to the earlier developmental stage of dissociated neuron cultures, whereas the trisynaptic hippocampal circuit was fully formed in slices from 1-month-old mice. The neuronal cultures also do not model glial-neuron interactions, as observed in conditioned media from mixed glia exposed to nPM, which altered neurite outgrowth (Morgan *et al.* 2011). The TNF-alpha secretion induced in mixed glia by nPM is a candidate for modulation of neurite outgrowth (Cheng *et al.* 2012), and for modulation of AMPA receptor subunits (Santello and Volterra 2012)

These electrophysiological studies indicate that nPM can directly alter post-synaptic functions in CA1 pyramidal neurons, which showed the greatest membrane vulnerability

by EthD-1 assay. Thus, acute exposure to nPM caused a large reduction (50%) of evoked EPSC amplitudes across a range of stimulus intensity with minor immediate impact on pre-synaptic neurotransmitter release. We suggest a role for the impaired phosphorylation of GluN2B receptor, which in turn phosphorylates GluA1 for trafficking and insertion into the post-synaptic membrane. A post-synaptic location of these changes is indicated by the normal paired-pulse facilitation at Schaeffer collateral synapses, implying maintenance of pre-synaptic transmitter release. The paired-pulse plasticity expressed with synapses activated at short interstimulus intervals is a measure of neurotransmitter release (Fioravante and Regehr 2011). An alternative mechanism, which was not investigated, could involve effects of post-synaptically generated $NO^{\cdot}$ on the excitability of pre-synaptic terminals. Pilot data suggest greater alteration of NMDA receptor currents (Davis *et al.* 2012). Because of the importance of $NO^{\cdot}$-dependent GluA1 phosphorylation to memory (Traynelis *et al.* 2010), we predict that long-term potentiation LTP will be impaired by nPM exposure. For example, LTP is impaired in the mouse GluA1 S845A mutant that cannot be phosphorylated (Lee *et al.* 2010).

To develop a working model, we need to know if nPM exposure induces a cascade starting with Ca^{2+} influx from nPM that causes glutamate release, leading to induction of $NO^{\cdot}$. The role of long-lived free radicals in the nPM suspension (Morgan *et al.* 2011) to the induced cellular free radicals also remains unknown. Synapse-independent glutamate release can occur at neuritic growth cones (Soeda *et al.* 1997; Gelsomino *et al.* 2013). Further downstream may be remodeling of glutamate receptors through nitrosylation and phosphorylation of subunits via pathways that are recognized in LTP. This cascade is applicable to *in vivo* responses to chronic nPM inhalation initiated by neurons and glial in the olfactory mucosa, which project into the forebrain (Block and Calderon-Garciduenas 2009) and which transport synthetic nPM as far as the hippocampus and cerebellum (Oberdörster *et al.* 2004).

The present *in vitro* models do not address the putatively slower adaptive responses to nPM during chronic exposure *in vivo*, in which GluA1 was decreased (Morgan *et al.* 2011), in contrast to GluA1 increases from acute *in vitro* exposure. The present *in vitro* models of hippocampal slice and neuronal cultures give a basis for dissecting acute effects of nPM on neurons and glia of the nasal mucosa neuroepithelium and the olfactory bulb, which are the initial brain cell contacts of inhaled nPM (Oberdörster *et al.* 2004; Block and Calderon-Garciduenas 2009).

Lastly, we note potential links of nPM to brain aging and Alzheimer disease (AD) through glutamatergic functions and the amyloid β-peptide (Aβ). Human brains from a highly polluted city showed premature elevations of Aβ (Calderon-Garciduenas *et al.* 2012). In a rat model, chronic inhalation of diesel exhaust PM2.5 increased brain amyloid β-peptide (endogenous rat Aβ) (Levesque *et al.* 2011a). Ongoing epidemiological studies address possible associations of air pollution with AD and other dementias. Moreover, glutamate receptors have direct links to Aβ in rodent models. In AD transgenic (ADtg) mice carrying human Aβ, activation of metabotropic glutamate receptors promoted synaptic release of Aβ (Kim *et al.* 2010), whereas the FDA-approved, NMDA receptor antagonist Memantine decreased the brain Aβ load (Alley *et al.* 2010). Furthermore, activation of extrasynaptic NMDA receptors (predominantly GluN2B) increased $NO^{\cdot}$ and caused synapse loss (Talantova *et al.* 2013). Thus, the hippocampal spine loss from inhalation of PM observed in mice exposed to diesel PM2.5 (Fonken *et al.* 2011) could involve the endogenous mouse Aβ, $NO^{\cdot}$, and glutamate. The newer NMDAR antagonist, NitroMemantine, protected against Aβ-induced synapse loss, as well as induction of $NO^{\cdot}$ and S-nitrosylation (Talantova *et al.* 2013). Future studies may consider therapeutic interventions with NMDAR antagonists on the synergies between nPM inhalation and Aβ as factors in cognitive impairments associated with aging, as well as onset and progression of AD.

Acknowledgements

Nahoko Iwata gave excellent assistance in western blots. We thank Michel Baudry, Enrique Cadenas, and Henry Forman for critical comments. This research was supported by grants to C.E. Finch from the NIH (AG-040683; AG-040753) and the USC Collaborative Research Fund, and to C. Sioutas South Coast Air Quality Management District (SCAQMD, award #11527). D.A. Davis was supported by NIA training Grant (T32 AG000037).

Authors Contributions

David A. Davis, acute hippocampal slices, neuronal cultures, western blots, nitric oxide, and superoxide assays, viability assays; Garnik Akopian, electrophysiology; John P. Walsh, electrophysiology; Constantinos Sioutas, nPM collections and administration; Todd E. Morgan and Caleb E. Finch, experimental design and analysis.

Supporting information

Additional supporting information may be found in the online version of this article at the publisher's web-site:

Figure S1. Representative westerns blots from CA1 and DG lysates of hippocampal slices incubated in nPM for 2h from a single experiment.

Figure S2. Hippocampal neuron cell culture responses to nPM.

Figure S3. Immunoprecipitation of CA1 neuron nitrosylated glutamate receptors.

Figure S4. AP5 blocked nPM mediated cell injury to hippocampal neurons.

Table S1. Antibodies

Table S2. Hippocampal slice synaptic protein response to nPM

References

Aizenman E., Lipton S. A. and Loring R. H. (1989) Selective modulation of NMDA responses by reduction and oxidation. *Neuron* **2**, 1257–1263.

Aizenman E., Hartnett K. A. and Reynolds I. J. (1990) Oxygen free radicals regulate NMDA receptor function via a redox modulatory site. *Neuron* **5**, 841–846.

Akopian G., Crawford C., Beal M. F., Cappelletti M., Jakowec M. W., Petzinger G., Gheorghe S. L., Chow R. and Walsh J. P. (2008) Decreased striatal dopamine release underlies increased expression of long-term synaptic potentiation at corticostriatal synapses 24 hours after 3-nitropropionic acid induced chemical hypoxia. *J Neurosci.* **28**, 9585–9597.

Akopian G. and Walsh J. P. (2002) Corticostriatal paired-pulse potentiation produced by voltage-dependent activation of NMDA receptors and L-type Ca(2+) channels. *J. Neurophysiol.* **87**, 157–165.

Alley G. M., Bailey J. A., Chen D., Ray B., Puli L. K., Tanila H., Banerjee P. K. and Lahiri D. K. (2010) Memantine lowers amyloid-beta peptide levels in neuronal cultures and in APP/PS1transgenic mice. *J. Neurosci. Res.* **88**, 143–154.

Baez M. V., Oberholzer M. V., Cercato M. C., Snitcofsky M., Aguirre A. I. and Jerusalinsky D. A. (2013) NMDA receptor subunits in the adult rat hippocampus undergo similar changes after 5 minutes in an open field and after LTP induction. *PLoS ONE* **8**, e55244.

Banker G. A. and Cowan W. M. (1977) Rat hippocampal neurons in dispersed cell culture. *Brain Res.* **126**, 397–425.

Block M. L. and Calderon-Garciduenas L. (2009) Air pollution: mechanisms of neuroinflammation and CNS disease. *Trends Neurosci.* **32**, 506–516.

Calderon-Garciduenas L., Solt A. C., Henriquez-Roldan C. *et al.* (2008) Long-term air pollution exposure is associated with neuroinflammation, an altered innate immune response, disruption of the blood-brain barrier, ultrafine particulate deposition, and accumulation of amyloid beta-42 and alpha-synuclein in children and young adults. *Toxicol. Pathol.* **36**, 289–310.

Calderon-Garciduenas L., Kavanaugh M., Block M. *et al.* (2012) Neuroinflammation, hyperphosphorylated tau, diffuse amyloid plaques, and down-regulation of the cellular prion protein in air pollution exposed children and young adults. *J. Alzheimers Dis.* **28**, 93–107.

Chen J. C. and Schwartz J. (2009) Neurobehavioral effects of ambient air pollution on cognitive performance in US adults. *Neurotoxicology* **30**, 231–239.

Cheng H., Morgan T. E. and Finch C. E. (2012) Nanoscale urban air pollutants inhibit neurite outgrowth via TNF alpha. Soc Neurosci Ann Meeting 2012 Abstract 189.19.

Daher N., Hasheminassab S., Shafer M. M., Schauer J. J. and Sioutas C. (2013). Seasonal and spatial variability in chemical composition and mass closure of ambient ultrafine particles in the megacity of Los Angeles. *Environ. Sci. Process. Impacts* **15**, 283–295.

Davis D. A., Akopian G., Sioutas C., Walsh J. P., Morgan T. E. and Finch C. E. (2012) Nano-particulates from urban vehicular exhaust decrease glutamate receptor function. Soc Neurosci Ann Meet 2012 Abstract 189.13.

Fioravante D. and Regehr W. G. (2011) Short-term forms of presynaptic plasticity. *Curr. Opin. Neurobiol.* **21**, 269–274.

Fonken L. K., Xu X., Weil Z. M., Chen G., Sun Q., Rajagopalan S. and Nelson R. J. (2011) Air pollution impairs cognition, provokes depressive-like behaviors and alters hippocampal cytokine expression and morphology. *Mol. Psychiatry* **16**(987–995), 973.

Frade J. G., Barbosa R. M. and Laranjinha J. (2009) Stimulation of NMDA and AMPA glutamate receptors elicits distinct concentration dynamics of nitric oxide in rat hippocampal slices. *Hippocampus* **19**, 603–611.

Geiser M., Rothen-Rutishauser B., Kapp N. *et al.* (2005) Ultrafine particles cross cellular membranes by nonphagocytic mechanisms in lungs and in cultured cells. *Environ. Health Perspect.* **113**, 1555–1560.

Gelsomino G., Menna E., Antonucci F. *et al.* (2013) Kainate induces mobilization of synaptic vesicles at the growth cone through the activation of protein kinase A. *Cereb. Cortex* **23**, 531–541.

Gillespie P., Tajuba J., Lippmann M., Chen L. C. and Veronesi B. (2013) Particulate matter neurotoxicity in culture is size-dependent. *Neurotoxicology* **36**, 112–117. doi:10.1016/j.neuro.2011.10.006.

Hara M. R., Agrawal N., Kim S. F. *et al.* (2005) S-nitrosylated GAPDH initiates apoptotic cell death by nuclear translocation following Siah1 binding. *Nat. Cell Biol.* **7**, 665–674.

Ignarro L. J., Fukuto J. M., Griscavage J. M., Rogers N. E. and Byrns R. E. (1993) Oxidation of nitric oxide in aqueous solution to nitrite but not nitrate: comparison with enzymatically formed nitric oxide from L-arginine. *Proc. Natl Acad. Sci. USA* **90**, 8103–8107.

Kawasaki K., Traynelis S. F. and Dingledine R. (1990) Different responses of CA1 and CA3 regions to hypoxia in rat hippocampal slice. *J. Neurophysiol.* **63**, 385–394.

Kim S. H., Fraser P. E., Westaway D. and St. George-Hyslop, P.H., Ehrlichm M.E., Gandy, S. (2010) Group II metabotropic glutamate receptor stimulation triggers production and release of Alzheimer's amyloid(beta)42 from isolated intact nerve terminals. *J. Neurosci.* **30**, 3870–3875.

Kleinman M. T., Araujo J. A., Nel A., Sioutas C., Campbell A., Cong P. Q., Li H. and Bondy S. C. (2008) Inhaled ultrafine particulate matter affects CNS inflammatory processes and may act via MAP kinase signaling pathways. *Toxicol. Lett.* **178**, 127–130.

Lee H. K., Takamiya K., He K., Song L. and Huganir R. L. (2010) Specific roles of AMPA receptor subunit GluR1 (GluA1) phosphorylation sites in regulating synaptic plasticity in the CA1 region of hippocampus. *J. Neurophysiol.* **103**, 479–489.

Levesque S., Taetzsch T., Lull M. E. *et al.* (2011a) Diesel exhaust activates and primes microglia: air pollution, neuroinflammation, and regulation of dopaminergic neurotoxicity. *Environ. Health Perspect.* **119**, 1149–1155.

Levesque S., Surace M. J., McDonald J. and Block M. L. (2011b) Air pollution & the brain: Subchronic diesel exhaust exposure causes neuroinflammation and elevates early markers of neurodegenerative disease. *J. Neuroinflammation* **8**, 105–115.

Levesque S., Taetzsch T., Lull M. E., Johnson J. A., McGraw C. and Block M. L. (2013) The role of MAC1 in diesel exhaust particle-induced microglial activation and loss of dopaminergic neuron function. *J. Neurochem.* **125**, 756–765.

Li N., Wang M., Oberley T. D., Sempf J. M. and Nel A. E. (2002) Comparison of the pro-oxidative and proinflammatory effects of organic diesel exhaust particle chemicals in bronchial epithelial cells and macrophages. *J. Immunol.* **169**, 4531–4541.

Li N., Sioutas C., Cho A. *et al.* (2003) Ultrafine particulate pollutants induce oxidative stress and mitochondrial damage. *Environ. Health Perspect.* **111**, 455–460.

Li R., Navab M., Pakbin P. *et al.* (2013) Ambient ultrafine particles alter lipid metabolism and HDL anti-oxidant capacity in LDLR-null mice. *J. Lipid Res.* **54**(6), 1608–1615.

Lourenço C. F., Santos R., Barbosa R. M., Gerhardt G., Cadenas E. and Laranjinha J. (2011) In vivo modulation of nitric oxide concentration dynamics upon glutamatergic neuronal activation in the hippocampus. *Hippocampus* **21**, 622–630.

Ma T., Hoeffer C. A., Wong H., Massaad C. A., Zhou P., Iadecola C., Murphy M. P., Pautler R. G. and Klann E. (2011) Amyloid beta-induced impairments in hippocampal synaptic plasticity are

rescued by decreasing mitochondrial superoxide. *J. Neurosci.* **31**, 5589–5595.

Manzoni O., Prezeau L., Marin P., Deshager S., Bockaert J. and Fagni L. (1992) Nitric oxide-induced blockade of NMDA receptors. *Neuron* **8**, 653–662.

Misra C., Kim S., Shen S. and Sioutas C. (2002) A high flow rate, very low pressure drop impactor for inertial separation of ultrafine from accumulation mode particles. *J. Aerosol Sci.* **33**, 735–752.

Morgan T. E., Davis D. A., Iwata N. *et al.* (2011) Glutamatergic neurons in rodent models respond to nanoscale particulate urban air pollutants in vivo and in vitro. *Environ. Health Perspect.* **119**, 1003–1009.

Morrison J. H. and Hof P. R. (1997) Life and death of neurons in the aging brain. *Science* **278**, 412–419.

Ning Z., Geller M. D., Moore K. F., Sheesley R., Schauer J. J. and Sioutas C. (2007) Daily variation in chemical characteristics of urban ultrafine aerosols and inference of their sources. *Environ. Sci. Technol.* **41**, 6000–6006.

Oberdörster G., Sharp Z., Atudorei V., Elder A., Gelein R., Kreyling W. and Cox C. (2004) Translocation of inhaled ultrafine particles to the brain. *Inhal. Toxicol.* **16**, 437–445.

Power M. C., Weisskopf M. G., Alexeeff S. E., Coull B. A., Spiro A. III and Schwartz J. (2011) Traffic-related air pollution and cognitive function in a cohort of older men. *Environ. Health Perspect.* **119**, 682–687.

Power M. C., Weisskopf M. G., Alexeeff S. E., Wright R. O., Coull B. A., Spiro A. III and Schwartz J. (2013) Modification by hemochromatosis gene polymorphisms of the association between traffic-related air pollution and cognition in older men: a cohort study. *Environ. Health* **12**, 16.

Reyes R. C., Brennan A. M., Shen Y., Baldwin Y. and Swanson R. A. (2012) Activation of neuronal NMDA receptors induces superoxide-mediated oxidative stress in neighboring neurons and astrocytes. *J. Neurosci.* **32**, 12973–12978.

Ryan T. J., Kopanitsa M. V., Indersmitten T. *et al.* (2013) Evolution of GluN2A/B cytoplasmic domains diversified vertebrate synaptic plasticity and behavior. *Nat. Neurosci.* **16**, 25–32.

Santello M. and Volterra A. (2012) TNFalpha in synaptic function: switching gears. *Trends Neurosci.* **35**, 638–647.

Santos S. D., Carvalho A. L., Caldeira M. V. and Duarte C. B. (2009) Regulation of AMPA receptors and synaptic plasticity. *Neuroscience* **158**, 105–125.

Sardar S. B., Philip M., Mayo P. R. and Sioutas C. (2005) Size-fractionated measurements of ambient ultrafine particle chemical composition in Los Angeles using the NanoMOUDI. *Environ. Sci. Technol.* **39**, 932–944.

Sattler R., Xiong Z., Lu W. Y., Hafner M., MacDonald J. F. and Tymianski M. (1999) Specific coupling of NMDA receptor activation to nitric oxide neurotoxicity by PSD-95 protein. *Science* **284**, 1845–1848.

Selvakumar B., Jenkins M. A., Hussain N. K., Huganir R. L., Traynelis S. F. and Snyder S. H. (2013) S-nitrosylation of AMPA receptor GluA1 regulates phosphorylation, single-channel conductance, and endocytosis. *Proc. Natl Acad. Sci. USA* **110**, 1077–1082.

Shi Z. Q., Sunico C. R., McKercher S. R., Cui J., Feng G. S., Nakamura T. and Lipton S. A. (2013) S-nitrosylated SHP-2 contributes to NMDA receptor-mediated excitotoxicity in acute ischemic stroke. *Proc. Natl Acad. Sci. USA* **110**, 3137–3142.

Soeda H., Tatsumi H. and Katayama Y. (1997) Neurotransmitter release from growth cones of rat dorsal root ganglion neurons in culture. *Neuroscience* **77**, 1187–1199.

Stein T. D., Anders N. J., DeCarli C., Chan S. L., Mattson M. P. and Johnson J. A. (2004) Neutralization of transthyretin reverses the neuroprotective effects of secreted amyloid precursor protein (APP) in APPSW mice resulting in tau phosphorylation and loss of hippocampal neurons: support for the amyloid hypothesis. *J. Neurosci.* **24**, 7707–7717.

Talantova M., Sanz-Blasco S., Zhang X. *et al.* (2013) Aβ induces astrocytic glutamate release, extrasynaptic NMDA receptor activation, and synaptic loss. *Proc. Natl Acad. Sci. USA* **110**, E2518–E2527.

Traynelis S. F., Wollmuth L. P., McBain C. J. *et al.* (2010) Glutamate receptor ion channels: structure, regulation, and function. *Pharmacol. Rev.* **62**, 405–496.

Weuve J., Puett R. C., Schwartz J., Yanosky J. D., Laden F. and Grodstein F. (2012) Exposure to particulate air pollution and cognitive decline in older women. *Arch. Intern. Med.* **172**, 219–227.

Win-Shwe T. T. and Fujimaki H. (2011) Nanoparticles and neurotoxicity. *Int. J. Mol. Sci.* **12**, 6267–6280.

Win-Shwe T. T., Mitsushima D., Yamamoto S., Fujitani Y., Funabashi T., Hirano S. and Fujimaki H. (2009) Extracellular glutamate level and NMDA receptor subunit expression in mouse olfactory bulb following nanoparticle-rich diesel exhaust exposure. *Inhal. Toxicol.* **21**, 828–836.

Win-Shwe T. T., Yamamoto S., Fujitani Y., Hirano S. and Fujimaki H. (2012) Nanoparticle-rich diesel exhaust affects hippocampal-dependent spatial learning and NMDA receptor subunit expression in female mice. *Nanotoxicology* **6**, 543–553.

Xia T., Kovochich M., Brant J. *et al.* (2006) Comparison of the abilities of ambient and manufactured nanoparticles to induce cellular toxicity according to an oxidative stress paradigm. *Nano Lett.* **6**, 1794–1807.

Xie Z., Wei M., Morgan T. E., Fabrizio P., Han D., Finch C. E. and Longo V. D. (2002) Peroxynitrite mediates neurotoxicity of amyloid beta-peptide1-42- and lipopolysaccharide-activated microglia. *J. Neurosci.* **22**, 3484–3492.

Zanchi A. C., Fagundes L. S., Barbosa F. Jr, Bernardi R., Rhoden C. R., Saldiva P. H. and do Valle A. C. (2010) Pre and post-natal exposure to ambient level of air pollution impairs memory of rats: the role of oxidative stress. *Inhal. Toxicol.* **22**, 910–918.

Zhang H., Liu H., Davies K. J., Sioutas C., Finch C. E., Morgan T. E. and Forman H. J. (2012) Nrf2-regulated phase II enzymes are induced by chronic ambient nanoparticle exposure in young mice with age-related impairments. *Free Radic. Biol. Med.* **52**, 2038–2046.

Zhao Y., Usatyuk P. V., Gorshkova I. A. *et al.* (2009) Regulation of COX-2 expression and IL-6 release by particulate matter in airway epithelial cells. *Am. J. Respir. Cell Mol. Biol.* **40**, 19–30.

Zielonka J. and Kalyanaraman B. (2010) Hydroethidine- and MitoSox-derived red fluorescence is not a reliable indicator of intracellular superoxide formation: another inconvenient truth. *Free Radic. Biol. Med.* **48**, 983–1001.

Title:
Urban air pollutants reduce synaptic function of CA1 neurons *via* an NMDA/NO$^{\cdot}$ pathway *in vitro.*

Authors:
David A. Davis[1], Garnik Akopian[1], John P. Walsh[1], Constantinos Sioutas[2], Todd E. Morgan[1] and Caleb E. Finch[1, 3]

Institution:
University of Southern California, Los Angeles, CA 90089

Affiliations:
[1]Davis School of Gerontology, [2]Viterbi School of Engineering, [3]Dept. of Neurobiology, Dornsife College, University of Southern California, Los Angeles, CA 90089

Address correspondence to:
Caleb E. Finch, PhD
3715 McClintock Avenue
University of Southern California
Los Angeles, CA 90089
213-740-1758 (voice)
213-740- 6581 (FAX)
cefinch@usc.edu

SUPPLEMENTAL INFORMATION

Figure S1:

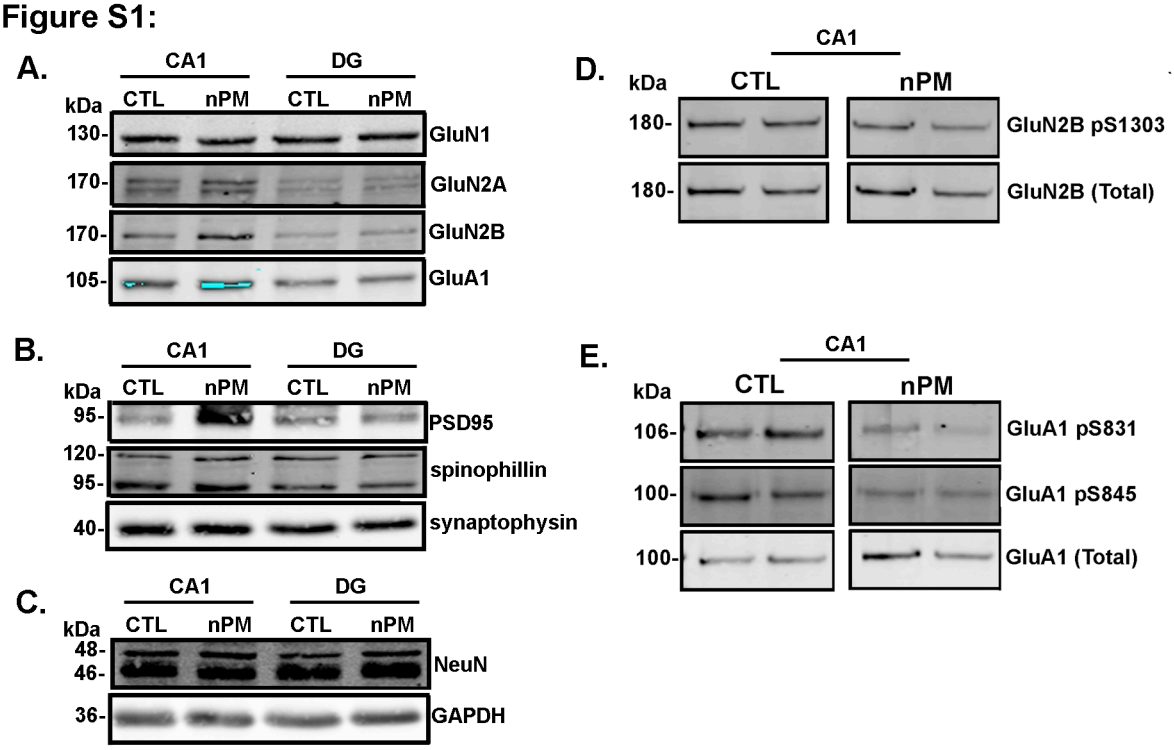

Figure S1: Representative Westerns blots from CA1 and DG lysates of hippocampal slices incubated in nPM for 2h from a single experiment. (A) Glutamate receptors, AMPA and NMDA receptor subunits; (B) Synaptic proteins; (C) NeuN and GAPDH, as loading controls; (D, E) Total and phosphorylated glutamate receptor proteins.

Figure S2:

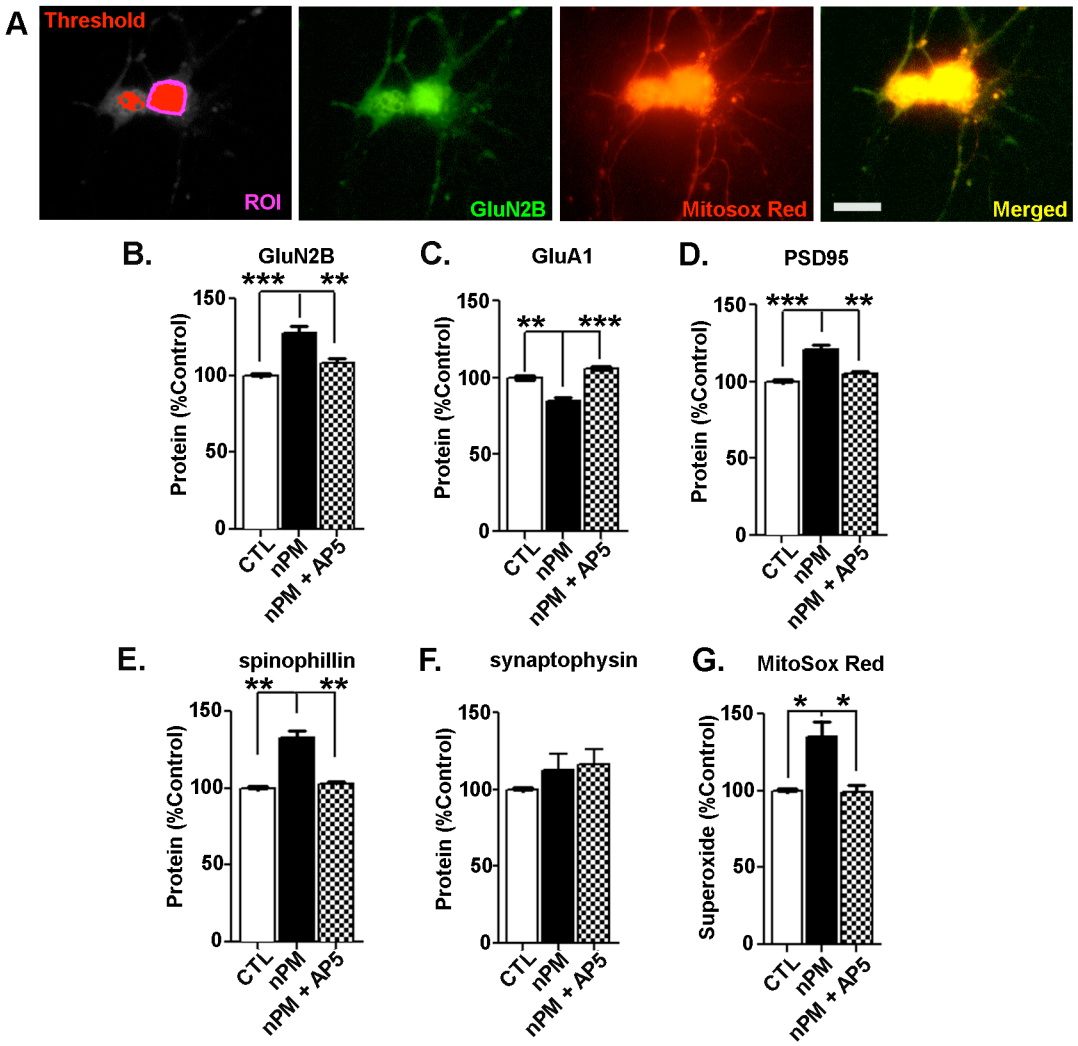

Figure S2: Hippocampal neuron cell culture responses to nPM

Rat primary hippocampal neuron cultures (E18) were exposed to nPM (10 µg/ml, 2 h) and immunostained. (A) Representative images of the NMDA receptor subunit GluN2B (green) and Mitosox Red (red). Immunofluorescence was measured in the perikaryal region of pyramidal neurons (ROI; purple); scale bar, 10 µm. (B-G): Western blot analysis of nPM effects on select proteins and effects of AP5. (B) GluN2B, +20%; (C) GluA1, -20%; (D) PSD95, +20%; (E) spinophilin, +30%; (F) synaptophysin, no change; (G) Mitosox™ Red, +40%. All nPM effects were blocked by AP5 (50µM); *p<0.05; **p<0.01; ***p<0.001.

Figure S3:

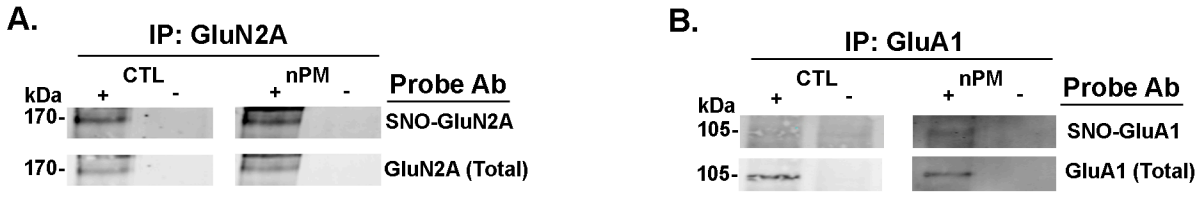

Figure S3: Immunoprecipitation of CA1 neuron nitrosylated glutamate receptors.

After incubation of hippocampal slices with nPM for 2 h (Figure 4C), glutamate receptor subunits were immunoprecipitated (IP), separated by electrophoresis and detected with an antibody to S-nitrosylation by Western blot to confirm the specificity of cysteine nitrosylation (Fig. 4C). (+) Indicates addition of IP antibody. (-) Indicates no IP antibody added to reaction.

(A) NMDA receptor subunit GluN2A IP. (B) AMPA receptor subunit GluA1 IP. Both showed higher nitrosylation of the specific band, consistent with the total protein nitrosylation (Figure 4C).

Figure S4:

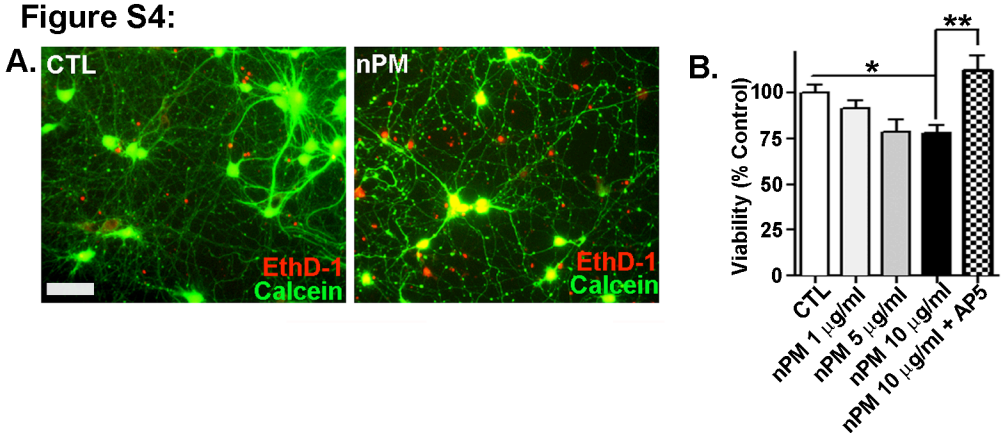

Figure S4: AP5 blocked nPM mediated cell injury to hippocampal neurons. Primary cultures of rat hippocampal neurons exposed to nPM (10 µg/ml nPM, 2 h) (A) LIVE/DEAD® assay for neuron viability: calcein AM (green) and Ethidium homodimer 1 (EthD-1; red); scale bar, 20 µm. nPM induced elevated uptake of EthD1 and neuritic beading; (B) EthD-1 uptake was dose-dependent and blocked by AP5; *p<0.05; **p<0.01.

Table S1: Antibodies

Antigen Target	Antigen Sequence	Antibody	Manufacture / Catalogue no.	Species	Dilution
Actin	C-terminal peptide	Anti-Actin AC-40	Sigma-Aldrich/ A3853	Mouse Monoclonal	1;10,000-WB
CD11b	Peritoneal macrophages	Rat Anti Mouse CD11b	Serotec/ MCA711	Rat Monoclonal	1:500-WB
GluA1	C-terminus (A.A. Region 850)	Glutamate Receptor 1 (AMPA Subtype)	Abcam/ AB31232	Rabbit Polyclonal	1; 1,000-WB 1; 200-ICC
GluA1 pS831	Phospho S831	Phopho-GluR1(S831) clone N453	Millipore/ 04-823	Rabbit Polyclonal	1; 1,000-WB
GluA1 pS845	PhosphoS845	Glutamate Receptor 1 Phospho S845	Millipore/ AB5849	Rabbit Polyclonal	1; 1,000-WB
GluA2	BSA-C-GluA2(C-Terminus)	Glutamate Receptor 2	Millipore/ AB1768	Rabbit Polyclonal	1;2,000-WB
mGluR5	mGluR5(N-Terminus)	Metabotropic Glutamate Receptor 5	Abcam/ AB53090	Rabbit Polyclonal	1;1,000-WB
GluN1	HIS-NR1A (A.A. 834-938)	NR1, CT	Millipore/ 05-432	Mouse Monoclonal	1;1,000-WB
GluN2A	HIS NR2A (A.A. 1265-1464)	NR2A	Millipore/ 07-632	Rabbit Polyclonal	1;1,000-WB
GluN2B	NR2B (A.A. 1437-1456)	NR2B	Millipore/ 06-600	Rabbit Polyclonal	1;1,000-WB
GluN2B pS1303	KLH-NR2B (A.A. 1297-1309) with Phospho A.A. SER 1303	Phospho-NR2B (Ser1303)	Upstate/ 07-398	Rabbit Polyclonal	1;1,000-WB
IbA1	IbA1 protein	Anti IbA1, Rabbit	Wako/ 016-20001	Rabbit Polyclonal	1;200-IHC
PSD95	Recombinant PSD95.	[6G6-1C9] to PSD95	Millipore/ AB2723	Mouse Monoclonal	1;1,000-WB
synaptophysin	Whole Molecule	synaptophysin	Millipore/ MAB368	Mouse Monoclonal	1;5,000-WB 1;200-ICC
spinophilin	GST-spinophilin (A.A. 286-390)	spinophilin/neurabin II	Millipore/ 06-852	Rabbit polyclonal	1;1,000-WB 1;200-ICC
SNO-Cys-Proteins	S-Nitro-Cysteine-KLH	S-Nitro-Cysteine (SNO-CYS)	Sigma-Aldrich/ N5411	Rabbit Polyclonal	1;1,000-WB
NeuN	Cell Nuclei	NeuN, Clone A60	Millipore/ MAB377	Mouse Monoclonal	1;500-WB 1:100-IHC
GAPDH	Whole Molecule	GAPDH	Ambion/ AM4300	Mouse Monoclonal	1;10,000-WB
GFAP	Purified Pig GFAP from spinal cord	Anti-Glial Fibrillary Acidic Protein (GFAP) Clone GA5	Sigma-Aldrich/G3893	Mouse Monoclonal	1:1,000-WB 1:400-IHC
mouse or rabbit or rat IgG	IgG-Heavy and Light Chain	IRDye 800 or 680 CW	LI-COR Biosciences/ 92632210	Goat Polyclonal	1:10,000-WB
mouse or rabbit IgG	IgG-Heavy and Light Chain	Alexa Fluor® 594 or 488	Molecular Probes/ A11032 or A11034	Goat Polyclonal	1:400-ICC 1:200-IHC

ICC= Immunocytochemistry; IHC= Immunohistochemistry; WB=Western blot

Table S2: Hippocampal slice synaptic protein response to nPM

	CA1 region		**DG region**	
Antigen	**% change.**	***P*< value**	**% change**	***P*< value**
NMDA				
GluN1	10 ± 5	NS	20 ± 26	NS
GluN2A	60± 19	<0.05	30 ± 9	NS
GluN2B	80 ± 19	<0.05	5 ± 13	NS
GluN2B pS1303	-30 ± 2	<0.001	-20 ± 17	NS
Non-NMDA				
GluA1	70 ± 30	<0.05	14 ± 17	NS
GluA1 pS845	-40 ± 14	<0.05	0 ± 18	NS
GluA1 pS831	-40 ± 2	<0.05	-29 ± 16	NS
GluA2	30 ± 17	NS	10 ± 4	NS
mGluR5	22 ± 14	NS	30 ± 26	NS
Synaptic Proteins				
synaptophysin	-5 ± 10	NS	7 ± 9	NS
PSD95	100 ± 40	<0.05	-10 ± 18	NS
spinophilin	45 ± 6	<0.01	-10 ± 13	NS
Protein Nitrosylation				
SNO-GluN2A	40 ± 6	<0.01	-20 ± 15	NS
SNO-GluA1	50 ± 13	<0.05	-20 ± 9	NS
SNO-GAPDH	50 ± 15	<0.01	17 ± 9	NS

Hippocampal slices were incubated 2 h with 10 µg/ml nPM. The CA1 pyramidal neuron layer and dentate gyrus (DG) neuron layer were microdissected from adjacent tissue and analyzed by Western blotting; NS, no significant change.